Absorption and backscattering coefficients and their relations to water constituents of Poyang Lake, China

Guofeng Wu,[1,*] Lijuan Cui,[2] Hongtao Duan,[3] Teng Fei,[1] and Yaolin Liu[1]

[1]School of Resource and Environmental Science & Key Laboratory of Geographic Information System of the Ministry of Education, Wuhan University, 430079, Wuhan, China

[2]Institute of Wetland Research, Chinese Academy of Forestry, 100091, Beijing, China

[3]State Key Laboratory of Lake Science and Environment, Nanjing Institute of Geography and Limnology, Chinese Academy of Sciences, 210008, Nanjing, China

*Corresponding author: guofeng.wu@whu.edu.cn

Received 3 June 2011; revised 30 September 2011; accepted 6 October 2011; posted 12 October 2011 (Doc. ID 148611); published 25 November 2011

The measurement and analysis of inherent optical properties (IOPs) of the main water constituents are necessary for remote-sensing-based water quality estimation and other ecological studies of lakes. This study aimed to measure and analyze the absorption and backscattering coefficients of the main water constituents and, further, to analyze their relations to the water constituent concentrations in Poyang Lake, China. The concentrations and the absorption and backscattering coefficients of the main water constituents at 47 sampling sites were measured and analyzed as follows. (1) The concentrations of chlorophyll a (C_{CHL}), dissolved organic carbon (C_{DOC}), suspended particulate matter (C_{SPM}), including suspended particulate inorganic matter (C_{SPIM}) and suspended particulate organic matter (C_{SPOM}), and the absorption coefficients of total particulate (a_p), phytoplankton (a_{ph}), nonpigment particulate (a_d), and colored/chromophoric dissolved organic matter (a_g) were measured in the laboratory. (2) The total backscattering coefficients, including the contribution of pure water at six wavelengths of 420, 442, 470, 510, 590, and 700 nm, were measured in the field with a HydroScat-6 backscattering sensor. (3) The backscattering coefficients without the contribution of pure water (b_b) were then derived by subtracting the backscattering coefficients of pure water from the total backscattering coefficients. (4) The C_{CHL}, C_{SPM}, C_{SPIM}, C_{SPOM}, and C_{DOC} of the 41 remaining water samples were statistically described and their correlations were analyzed. (5) The a_{ph}, a_d, a_p, a_g, and b_b were visualized and analyzed, and their relations to C_{CHL}, C_{SPM}, C_{SPIM}, C_{SPOM}, or C_{DOC} were studied. Results showed the following. (1) Poyang Lake was a suspended particulate inorganic matter dominant lake with low phytoplankton concentration. (2) One salient a_{ph} absorption peak was found at 678 nm, and it explained 72% of the variation of C_{CHL}. (3) The a_d and a_p exponentially decreased with increasing wavelength, and they explained 74% of the variation of C_{SPIM} and 71% variation of C_{SPM}, respectively, at a wavelength of 440 nm. (4) The a_g also exponentially decreased with increasing wavelength, and it had no significant correlation to C_{DOC} at a significance level of 0.05. (5) The b_b decreased with increasing wavelength, and it had strong and positive correlations to C_{SPM}, C_{SPIM} and C_{SPOM}, a strong and negative correlation to C_{CHL}, and no correlation to C_{DOC} at a significance level of 0.05. Such results will be helpful for the understanding of the IOPs of Poyang Lake. They, however, only represented the IOPs during the sampling time period, and more measurements and analyses in different seasons need to be carried out in the future to ensure a comprehensive understanding of the IOPs of Poyang Lake. © 2011 Optical Society of America

OCIS codes: 290.1350, 300.1030.

0003-6935/11/346358-11$15.00/0

1. Introduction

Inherent optical properties (IOPs) are the optical properties of water that are dependent on water and its constituents but independent of the ambient light field [1]. The most fundamental parameters of IOPs are the absorption and backscattering coefficients of the main water constituents [2]. IOPs influence the underwater light climate, which is an important factor controlling aquatic ecosystems [2–6]. The measurement of IOPs is also the foundation of parameterizing bio-optical models for monitoring water quality [1,7,8]. Thus, quantifying IOPs is necessary for studying the underwater light climate and for estimating water quality parameters in ecological studies.

Studies of IOPs have been carried out for many years. Open ocean waters (Case 1 waters), such as the Arabian Sea [9], Arctic Ocean [10], and Southern Ionian Sea [11], used to be the main focus [1], and, generally, their IOPs are well measured, analyzed, and understood for their simple optical properties. Recently, much attention has been paid to analyzing the IOPs of Case 2 waters in coastal oceans [12,13], lakes [1,5,14–16], estuaries [17], and reservoirs [18], because of their direct impacts on human activities [19].

The IOPs of Case 2 waters are dominated by three constituents: (a) phytoplankton, the biomass of which is generally estimated with chlorophyll *a* (CHL) concentration as a proxy, (b) suspended particulate matter (SPM), including suspended particulate inorganic matter (SPIM) and suspended particulate organic matter (SPOM), and (c) "yellow substance," also known as colored/chromophoric dissolved organic matter (CDOM), which is the major component of dissolved organic carbon (DOC) [8,20]. To quantify and understand the aggregate IOPs of Case 2 waters is a challenge because they are generally more optically complex than Case 1 waters, of which the IOPs are dominated by phytoplankton and its by-products [21].

Generally, the absorption coefficients of phytoplankton, SPM, and CDOM are measured in the laboratory using spectrophotometers [17,22,23]. Recently, field spectrophotometers, such as the AC-9 and AC-S (WET Labs Inc.), have been widely used for *in situ* measurements [10,17,18,22,24,25]. The accurate measurement of absorption coefficients in the field, however, is almost impossible because of the difficulty of designing sensors that fully collect all the scattered photons [3]. The backscattering coefficient of water is measured using a spectral backscattering sensor, such as the HydroScat-6 (HOBI Labs) and ECO-BB9 (WET Labs Inc.) [4,18,26,27], and it can also be estimated from the attenuation and absorption coefficients measured with spectrophotometers [3].

There are numerous lakes widely distributed in China, and their total area is around 81,000 km^2 [28]. Currently, many of these lakes are facing a number of problems, such as a decrease in lake area and water quality decline caused by natural or anthropogenic factors, which might hamper the sustainable development of lake functions [25]. Absorption and backscattering coefficients have been measured and analyzed in several Chinese lakes, such as Taihu Lake [29–33] and Chaohu Lake [34]; however, the IOPs of most Chinese lakes are still unknown.

Poyang Lake is the largest freshwater lake in China, and it provides multiple functions to society, through production, recreation, and biodiversity conservation. The provision of these functions is greatly influenced by water quality. However, the IOPs of Poyang Lake have rarely been measured and analyzed (we do know that Jiangxi Normal University carried out IOP studies on Poyang Lake, but no published work was found from our literature review). This study aims to estimate the absorption and backscattering coefficients of the water body, and, further, to analyze their relations to the main water constituents in Poyang Lake. This will provide help for remote-sensing-based monitoring of water quality and other ecological studies of Poyang Lake.

2. Materials and Methods

A. Study Area

Poyang Lake (115°47′–116°45′E, 28°22′–29°45′N) is located south of the middle reaches of the Yangtze River (Fig. 1). It receives water from five rivers (Raohe, Xinjiang, Fuhe, Ganjiang, and Xiushui) and drains into the Yangtze through a channel in the north. Its size fluctuates from less than 1000 km^2 in the dry season to around 4000 km^2 in the flood season [35–37]. Poyang Lake is an important international wetland with a rich biodiversity of 102 species of aquatic plants and 122 species of fish. It is also one of the largest bird conservation areas in

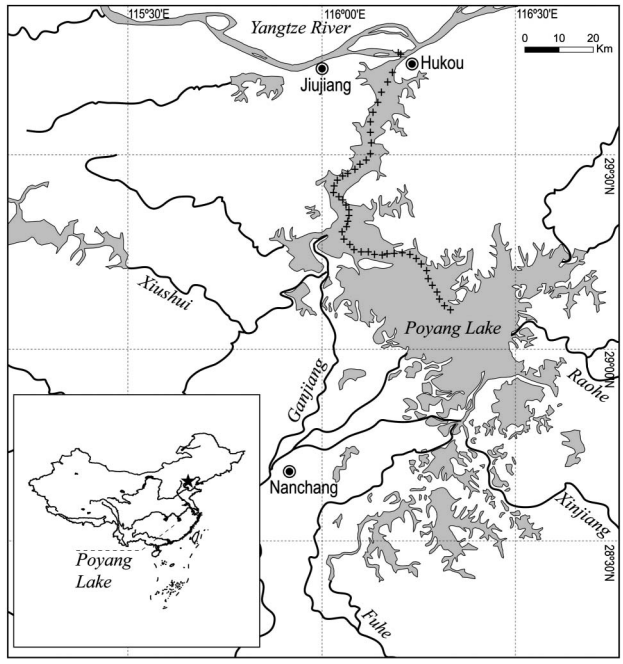

Fig. 1. Map showing the location of Poyang Lake and the sampling sites (black crosses).

the world, hosting millions of birds from over 300 species [38]. Poyang Lake has a significant role in local economic and social development, as well as global ecological conservation [39].

With the increasing human population and the growth of intensive economic activities within the Poyang basin in recent decades, the nutrient levels of Poyang Lake (e.g., total nitrogen and total phosphorus concentrations) have shown a clear increasing trend. This is due to agricultural chemical inputs and industrial and waste discharges, which have resulted in severe eutrophication in some regions [40,41]. The intensive sand dredging activities, which started around 2001 in northern Poyang Lake [42], cause sediment to be resuspended and increase the sediment concentration [43]. Such water quality degradation greatly and negatively impacts the Poyang Lake ecosystem.

B. Data Collection

1. *Fieldwork*

Fieldwork was carried out on 16–18 October 2010 (only along the main river channel due to low water levels), and the locations, water samples, and water backscattering coefficients at 47 sampling sites (Fig. 1) were recorded, collected, and measured. At each sampling site, the geographical coordinates were recorded using a Garmin global positioning system (Garmin Ltd.), and about 1500 ml of surface water was collected at around 30–50 cm water depth and kept in a refrigerator for further measuring of the concentrations and absorption coefficients of the water constituents. The backscattering coefficient was measured with a HydroScat-6 backscattering sensor at around 30–50 cm water depth.

2. *Constituent Concentration*

A spectrophotometric determination method was used to measure chlorophyll a concentration (C_{CHL}): (a) the water sample was filtered using a Whatman GF/F glass fiber filter with 0.45 μm pore size and acetone was used to extract chlorophyll a from the filtered sample, (b) the sample was read before and after its acidification using a UV2401 spectrophotofluorometer (Shimadzu Corp.), and (c) C_{CHL} was calculated by comparing the readings with a known standard [44]. The SPM concentration (C_{SPM}) was measured gravimetrically as follows: (a) the water sample was filtered using a preweighted Whatman GF/F glass fiber filter with a 0.45 μm pore size, (b) the filter was dried for 2 h at 110 °C and reweighed after cooling to room temperature, (c) C_{SPM} was calculated through dividing the difference in filter weight after and before filtering by water sample volume, and (d) SPOM was removed from SPM by burning the filtered particulate at 550 °C for 3 h, and then the weights and concentrations of SPIM (C_{SPIM}) and SPOM (C_{SPOM}) were calculated [8]. A Model 1020 Total Organic Carbon Analyzer (O.I. Corp.) was used to measure DOC concentration (C_{DOC}) after the water sample was filtered using a Whatman GF/F glass fiber filter with a 0.45 μm pore size [8].

3. *Absorption Coefficient*

Ma *et al.* [8] described in detail the measurement and calculation of the absorption coefficients of total particulate (a_p), phytoplankton (a_{ph}), nonpigment particulate (a_d), and CDOM (a_g), while Laanen [45] discussed the impact of filtering pore size on absorption coefficients and concluded that the filtering pore size significantly contributed to the absorption measurements. These methods and results were considered when measuring the absorption coefficients in this study as follows: (a) the water sample was filtered using a Whatman GF/F glass fiber filter with a 0.7 μm nominal pore size; (b) the optical density of total particulate on the filter was measured using a UV-2401 spectrophotometer with 1 nm interval; (c) the optical density was normalized to zero at 750 nm, corrected for the increase in path length caused by multiple scattering in the glass fiber filter, and a_p was calculated using the equations of Cleveland and Weideman [46]; (d) after the optical density of total particulate was measured, the pigment was removed from the filtered paper by extracting with ethanol; (e) the optical density was measured again using the same spectrophotometer, and a_d was calculated with the same equations as mentioned in (c); (f) a_{ph} was derived by subtracting a_d from a_p; (g) the optical density of water filtered with a 0.22 μm polycarbonate filter was measured using the same spectrophotometer with distilled water as a reference, and a_g was calculated using the equation of Bricaud *et al.* [47] from the measured optical density and corrected with the equation of Keith *et al.* [48]

4. *Backscattering Coefficient*

A HydroScat-6 backscattering sensor was used to measure total backscattering coefficients, including the contribution of pure water at six wavelengths of 420, 442, 470, 510, 590, and 700 nm, under the guidance of the manual from HOBI Labs [49] as follows: (a) the sensor was calibrated before the field campaign, (b) at each sampling site, the sensor was immersed at around 30–50 cm water depth for at least 3 min, (c) the measured backscattering coefficients were examined to leave out exceptional data and the mean of the remaining measurements was calculated, (d) sigma correction was made to improve the accuracy of the backscattering measurements, in which the equipment default value of 0.015 was used as backscattering probability since there was no available information about backscattering probability in Poyang Lake, and (e) the backscattering coefficients, not including the contribution of pure water (b_b), were derived by subtracting the backscattering coefficients of pure water from the total backscatter-

ing coefficients. The detailed process and methods can be found in the literature of Ma *et al.* [8,31].

C. Data Analysis

The water samples with wrong measurements of absorption coefficient, backscattering coefficient, or constituent concentration were removed, and the absorption and backscattering coefficients of the remaining samples, as well as their relations to the main water constituents, were analyzed using STATISTICA (www.statsoft.com) and MATLAB software (http://www.mathworks.com).

1. *Constituent Concentration*

The C_{CHL}, C_{SPM}, C_{SPIM}, C_{SPOM}, and C_{DOC} of the remaining water samples were statistically described and their correlations were analyzed to explore the characteristics and relations of the important water constituents.

2. *Absorption Coefficient*

With 440 nm as a reference wavelength, the a_{ph}, a_d, and a_g were statistically described, and their contributions to total absorption (the sum of a_{ph}, a_d, and a_g) were analyzed.

The a_{ph} spectra were visualized and the typical diagnostic characteristics of phytoplankton were analyzed first. The correlation analysis between a_{ph} and C_{CHL} was then carried out. Finally, the regressions of a_{ph} against C_{CHL} at the two absorption peaks within wavelengths of 430–450 and 650–700 nm were created.

The a_d was visually analyzed, and the a_d spectra were simulated over the spectral range of 400–700 nm by using Eq. (1) with 440 nm as the reference wavelength [30]:

$$a_d(\lambda) = a_d(440)\exp(-S_d(\lambda - 440)), \quad (1)$$

where λ is the wavelength, $a_d(\lambda)$ means the a_d at λ, $a_d(440)$ is the a_d at 440 nm, and S_d is a parameter describing the shape of the regression curve between a_d and the wavelength. The correlation between a_d and C_{SPIM} was analyzed, and the regressions of a_d against C_{SPIM} and C_{CHL} at the reference wavelength of 440 nm were developed, respectively.

First, the a_p was visualized and analyzed, and then the correlation analysis between a_p and C_{SPM} was implemented. Finally, the regressions of a_p against C_{SPM} at the reference band of 440 nm and against C_{CHL} at the absorption peak within the wavelength of 650–700 nm were created, respectively.

The a_g was visually analyzed first, and then the a_g spectra were simulated over the spectral range of 400–700 nm by using Eq. (2) with 440 nm as the reference wavelength [30]:

$$a_g(\lambda) = a_g(440)\exp(-S_g(\lambda - 440)), \quad (2)$$

where λ is the wavelength, $a_g(\lambda)$ means the a_g at λ, $a_g(440)$ is the a_g at 440 nm, and S_g is a parameter describing the shape of the regression curve between a_g and the wavelength. The correlation analysis of a_g against C_{DOC} was carried out, and the regression of a_g against C_{DOC} was not developed because of the weak correlation between them. The correlations of a_g against C_{SPM}, C_{SPIM}, C_{SPOM}, and C_{CHL} were also analyzed.

3. *Backscattering Coefficient*

First the b_b was visualized and analyzed, and the correlation analyses between b_b and the main water constituents were then implemented at six wavelengths of 420, 442, 470, 510, 590, and 700 nm. Finally, the regressions of b_b against C_{SPM}, C_{SPIM}, C_{SPOM}, and C_{CHL} were created at the band with significantly highest correlation.

3. Results and Discussion

Six water samples were removed due to their wrong measurements of C_{CHL} (one sample with a negative value) or a_g (one sample with a negative value and four samples with wrong a_g curves), and, thus, only 41 samples remained for the following analyses.

A. Constituent Concentration

The statistical results of C_{CHL}, C_{SPM}, C_{SPIM}, C_{SPOM}, and C_{DOC} of all 41 water samples are shown in Table 1. The low average value ($C_{CHL} = 8.85\,\mu g/L$) with high variation (coefficient of variation = 72.43%) of C_{CHL} revealed that the lake was close to eutrophic status as a whole, while showing eutrophication ($C_{CHL} > 10\,\mu g/L$) in some regions. The SPM held a high average concentration value ($C_{SPM} = 55.72\,mg/L$) with high variation (coefficient of variation = 55.76%), in which SPIM (average $C_{SPIM} = 48.02\,mg/L$) occupied the dominant position when compared to SPOM (average $C_{SPOM} = 7.70\,mg/l$). Two sampling points with C_{SPM} of more than 100 mg/l were observed in Fig. 2(a), and they were close to sand dredging regions in which dredging actives cause the sediment to be resuspended and greatly increase the C_{SPM}. The DOC showed low concentration values (average $C_{DOC} = 3.02\,mg/l$) with low variation (coefficient of variation = 18.54%). The C_{CHL} and C_{DOC} were lower

Table 1. Statistics Describing the Concentrations of Chlorophyll *a* (C_{CHL}, $\mu g/l$), Suspended Particulate Matter (C_{SPM}, mg/l), Suspended Particulate Inorganic Matter (c_{spim}, mg/l), Suspended Particulate Organic Matter (c_{spom}, mg/l), and Dissolved Organic Carbon (c_{doc}, mg/l) of 41 Water Samples[a]

	C_{CHL}	C_{SPM}	C_{SPIM}	C_{SPOM}	C_{DOC}
Minimum	1.47	19.00	13.00	3.60	2.29
Maximum	24.65	168.00	148.00	20.00	4.36
Average	8.85	55.72	48.02	7.70	3.02
StdDev	6.41	31.07	28.27	3.15	0.56
CoeVar	72.43	55.76	58.87	40.91	18.54

[a]StdDev means standard deviation (unit is same as that of the above corresponding parameter), and CoeVar is coefficient of variation (%).

and C_{SPM} and C_{SPIM} were equivalent to or higher than that of Taihu Lake, China [27,30,50].

The correlation analyses among the main water constituent concentrations indicated a weak and negative correlation between C_{SPM} and C_{CHL} [$r = -0.44$, Fig. 2(a)] and noncorrelation between C_{DOC} and C_{CHL} [$r = 0.25$, Fig. 2(b)], as well as between C_{DOC} and C_{SPM} [$r = -0.09$, Fig. 2(c)] at a significance level of 0.05. Such weak or noncorrelation combined with the low C_{CHL} indicated the possibility that the SPM and CDOM were mainly from land-based sources or sediment resuspension but not from the degradation product of phytoplankton. The analyses also showed the strong and positive correlations among C_{SPM}, C_{SPIM}, and C_{SPOM} [$r = 0.99$, 0.90, and 0.88, Figs. 2(d)–2(f)] at a significance level of 0.001, which further indicated the dominant role of SPIM within SPM.

B. Absorption at 440 nm

Table 2 displays the statistical results on a_{ph}, a_d, and a_g and their contribution to total absorption of 41 water samples at a wavelength of 440 nm. a_d achieved the highest average value ($a_d = 4.5542\ m^{-1}$) with highest variation (coefficient of variation = 54.52%), and it occupied the dominant contribution (average contribution = 74%) to total absorption. a_{ph} showed moderate contribution with an average value of $0.8008\ m^{-1}$ and an average contribution of 15.10%, while a_g had the lowest value (average $a_g = 0.5581\ m^{-1}$ with a variation coefficient of 27.80%) and contribution (average contribution = 10.90%). Such results indicated that the IOPs of Poyang Lake were dominated by nonpigment particulate during the time period of sampling.

C. a_{ph}

Forty-one a_{ph} spectra at wavelengths of 400–700 nm are shown in Fig. 3(a). One salient absorption peak was found in the red range of 650–700 nm [Figs. 3(a) and 3(b)], which is consistent with the typical diagnostic characteristic of phytoplankton; while another absorption peak of phytoplankton in the blue range of 430–450 nm was not observed or was very inconspicuous [Figs. 3(a) and 3(b)], which might be explained by the low phytoplankton concentration [22,30]. Such a spectrum pattern is similar to that found in the Tamar estuary of the UK [17], but is quite different than that in Taihu Lake and Chaohu Lake of China [22,30], which generally show two obvious absorption peaks at the ranges of 430–450 and 650–700 nm.

The correlation analysis between a_{ph} and C_{CHL} [Fig. 3(c)] showed that the correlation coefficient (r) achieved the highest value at 439 nm ($r = 0.128$, $P = 0.4238$) and 678 nm ($r = 0.847$, $P < 0.001$) within the ranges of 430–450 and 650–700 nm, respectively. Such results are consistent with the phytoplankton absorption peaks close to 440 and 676 nm reported in many studies. The insignificant relation between a_{ph} and C_{CHL} at 439 nm [Fig. 3(d)] at a significance level of 0.05 might be because the a_{ph} is affected not only by chlorophyll a but also by other accessory pigments, such as carotenoid. The dominant contribution of chlorophyll a to a_{ph} at a wavelength of 678 nm results in the significantly linear relation between them at a significance level of

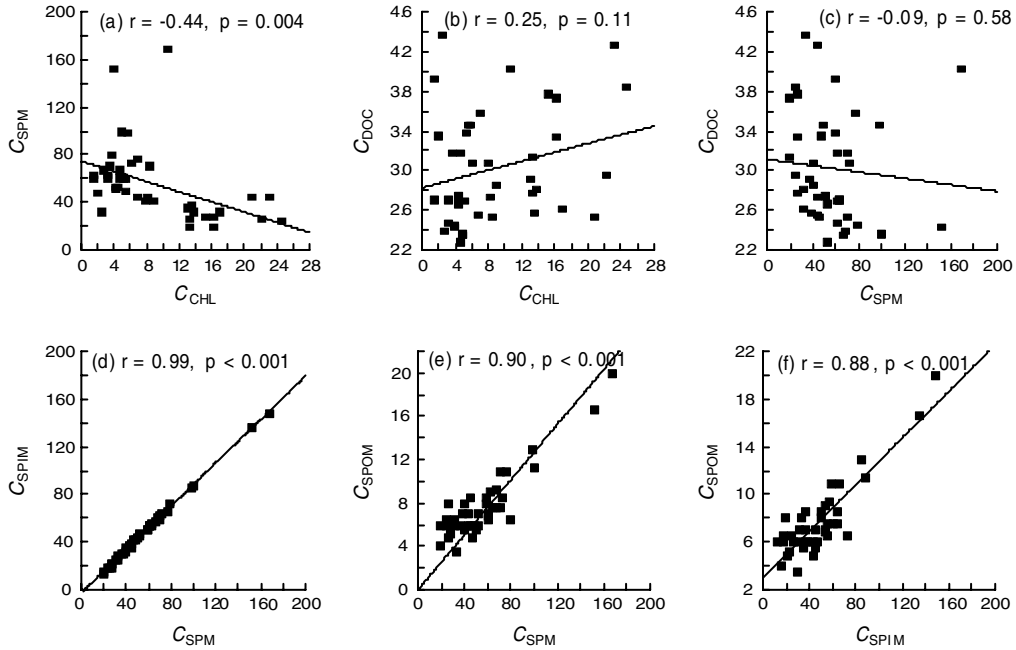

Fig. 2. Correlations among the concentrations of chlorophyll a (C_{CHL}, $\mu g/l$), suspended particulate matter (C_{SPM}, mg/l), suspended particulate inorganic matter (C_{SPIM}, mg/l), suspended particulate organic matter (C_{SPOM}, mg/l), and dissolved organic carbon (C_{DOC}, mg/l) of the 41 water samples. The black lines are the best fitting linear models between two of the main water constituent concentrations, and the intercept of linear fit in (e) was set as 0.

Table 2. Statistics Describing the Absorption Coefficient of Phytoplankton (a_{ph}, m^{-1}), Nonpigment Particulate (a_d, m^{-1}), and Dissolved Organic Carbon (a_g, m^{-1}) of 41 Water Samples at a Wavelength of 440 nm, and Their Corresponding Contributions to Total Absorption[a]

	a_{ph}	a_d	a_g	p_{ph}	p_d	p_g
Minimum	0.2953	1.2412	0.3277	6.93	53.33	4.13
Maximum	2.0142	10.4400	1.0067	36.72	86.83	21.43
Average	0.8008	4.5542	0.5581	15.10	74.00	10.90
StdDev	0.3057	2.4829	0.1552	6.92	9.58	4.69
CoeVar	38.17	54.52	27.80	45.83	12.95	43.02

[a] p_{ph}, p_d,and p_g are contributions (100%) of a_{ph}, a_d and a_g to total absorption. StdDev means standard deviation (unit is same as that of the above corresponding parameter), and CoeVar is coefficient of variation (%).

0.001 [Fig. 3(e)] [22,30,50,51], and the weak absorption of other accessory pigments, such as allophycocyanin, might explain why a_{ph} was not equal to zero when C_{CHL} came to zero [Fig. 3(e)].

D. a_d

All 41 a_d spectra showed a similar pattern, and they exponentially decreased along with the increasing wavelength at 400–700 nm [Fig. 4(a)]. This pattern is similar to that found in some water bodies, such as around the San Juan Islands of the USA [52], the Pearl River estuary [53], and Taihu Lake [30]. The S_d of the negative exponential function between a_d and the wavelength ranged from 0.0114 to 0.0175 nm^{-1} with a mean of $0.0142 \pm 0.0015\ nm^{-1}$,

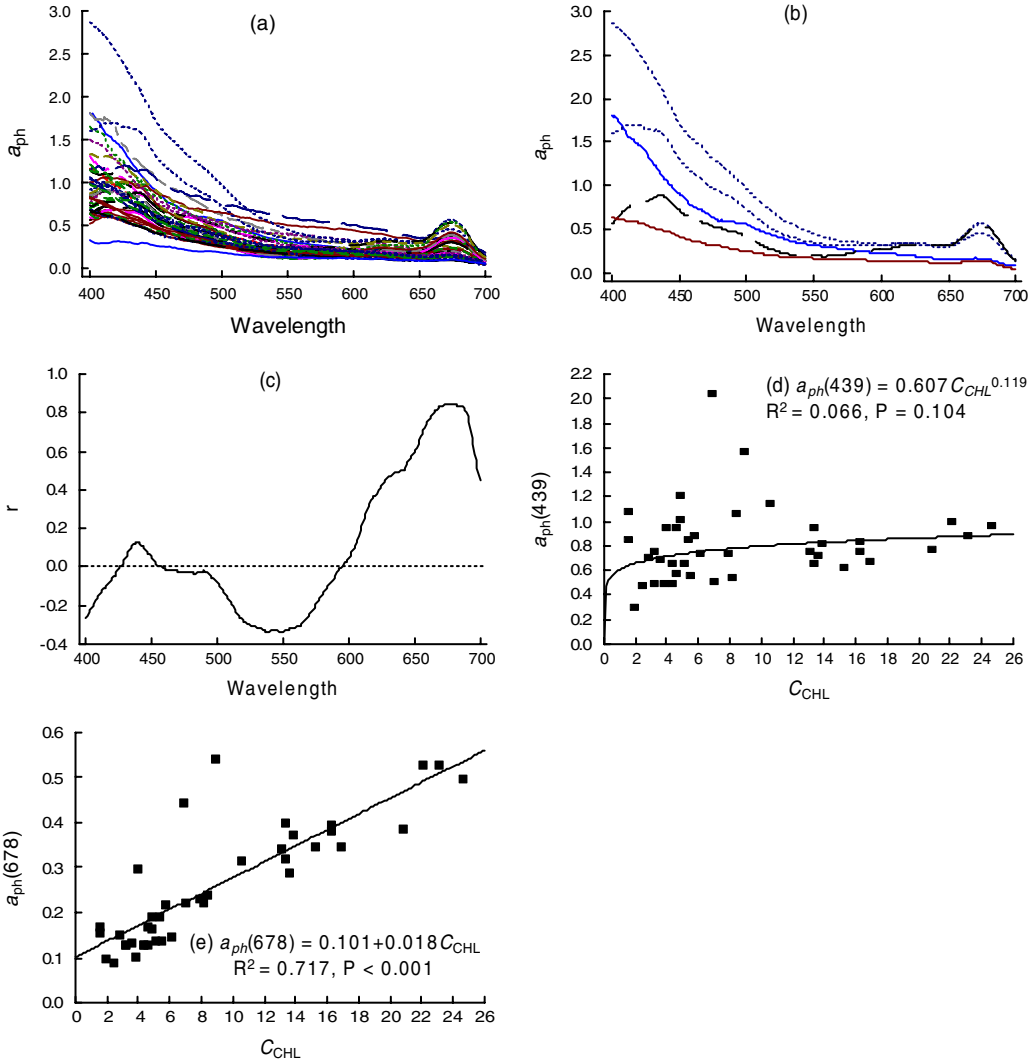

Fig. 3. (Color online) (a) Absorption coefficient of phytoplankton (a_{ph}, m^{-1}) at wavelengths of 400–700 nm for the 41 samples. (b) Absorption coefficient of phytoplankton (a_{ph}, m^{-1}) at wavelengths of 400–700 nm for typical samples. (c) Correlation (r) between a_{ph} and chlorophyll a concentration (C_{CHL}, $\mu g/l$). (d) Regression between C_{CHL} and a_{ph} at a wavelength of 439 nm ($a_{ph}(439)$). (e) Regression between C_{CHL} and a_{ph} at a wavelength of 678 nm [$a_{ph}(678)$].

which is higher than that of the San Juan Islands [52], Chaohu Lake, and Taihu Lake [30,54].

Strong and positive correlations existed between a_d and C_{SPIM} ($r = 0.79 \pm 0.02$) at wavelengths of 400–700 nm, especially at 400–500 nm ($r > 0.8$) [Fig. 4(b)]. The analyses further showed that the a_d at a wavelength of 440 nm ($a_d(440)$) ranged from 1.241 to 10.440 nm^{-1} with a mean of $4.554 \pm 2.483\ nm^{-1}$, and it increased with increasing C_{SPIM} following a power function [Fig. 4(c)] but exponentially decreased with increasing C_{CHL} [Fig. 4(d)].

E. a_p

Figure 5(a) displays the a_p at wavelengths of 400–700 nm, which includes the combined contributions of phytoplankton and nonpigment particulate. The a_p exponentially decreased with the increasing wavelength, and its pattern is similar to that of nonpigment particulate [Fig. 4(a)]. The two a_{ph} peaks within the ranges of 430–450 and 650–700 nm observed in Fig. 3(a) were not found in Fig. 5(a), and they were totally masked by a_d for the high concentration of nonpigment particulate. This pattern is quite different from that found in Taihu, Chaohu, and Xuanwuhu lakes of China [22], which generally show two obvious absorption peaks.

Because of the combined contributions of phytoplankton and nonpigment particulate, the correlation between a_p and C_{SPM} was strong at the wavelengths around 400–600 nm ($r >= 0.8$), declined from about 600 nm while reaching the lowest value at 678 nm ($r = 0.18$), and increased quickly at 678–700 nm [Fig. 5(b)]. Further analyses showed that the a_p also increased with increasing C_{SPM} following a power function at 440 nm [Fig. 5(c)] that is similar to that found in Fig. 4(c), while the C_{CHL} only explained around 31.5% variation of a_p at a wavelength of 678 nm [Fig. 5(d)], which is quite different when compared to the 71.7% variation of a_{ph} [Fig. 3(e)]. Such similarity and difference are mainly because of the dominant role of nonpigment particulate within the total particulate.

F. a_g

The a_g exponentially decreased with increasing wavelength at 400–700 nm [Fig. 6(a)], which is similar to a_d [Fig. 4(a)] and a_p [Fig. 5(a)]. This pattern is also similar to that found around the San Juan Islands [52] and Taihu Lake [30]. The S_g of the negative exponential function between a_g and wavelength ranged from 0.0096 to 0.0188 nm^{-1} with a mean of $0.0136 \pm 0.0022\ nm^{-1}$, which is equivalent to or lower than that found around the San Juan Islands [52], Taihu Lake [30], and some other water bodies in the world [30]. Such results indicated that S_g varied considering different water bodies, different seasons, or different parts of the same water body, and the different sources or constitutes of CDOM might result in this variation.

The correlation analyses between a_g and C_{DOC} [Fig. 6(b)] showed that the correlation coefficient achieved the lowest value at 439 nm ($r = 0.023$,

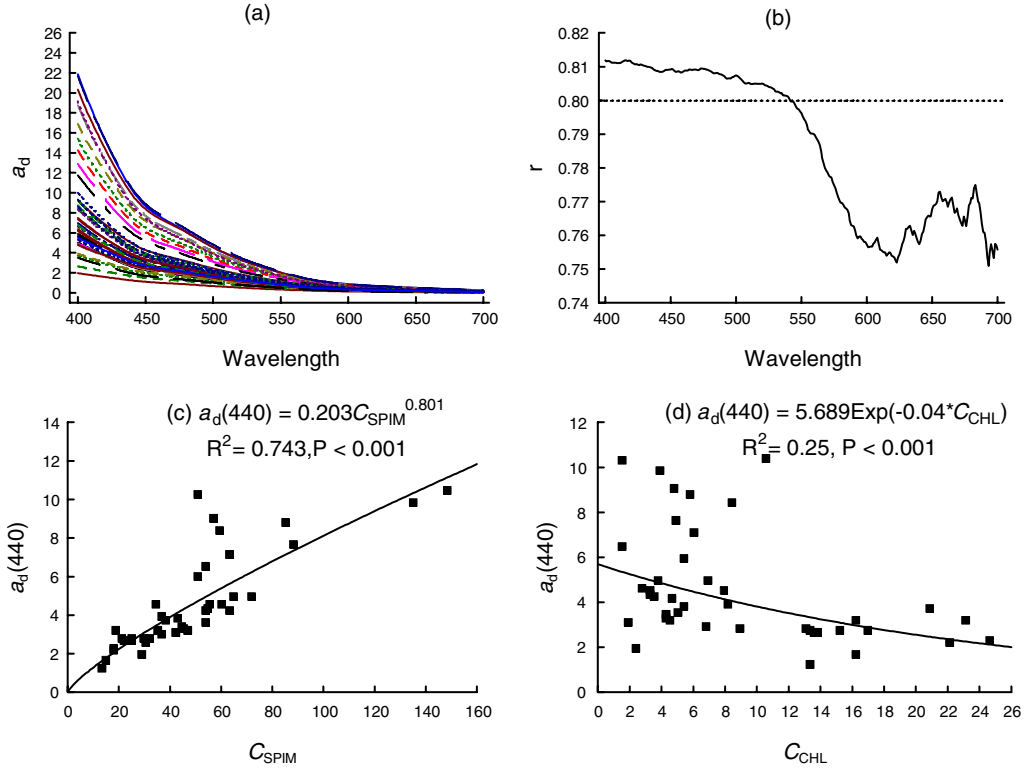

Fig. 4. (Color online) (a) Absorption coefficient of nonpigment particulate (a_d, m^{-1}) at wavelengths of 400–700 nm. (b) Correlation (r) between a_d and suspended particulate inorganic matter concentration (C_{SPIM}, mg/l). (c) Regression between C_{SPIM} and a_d at a wavelength of 440 nm [$a_d(440)$]. (d) Regression between chlorophyll a concentration (C_{CHL}, mg/l) and $a_d(440)$.

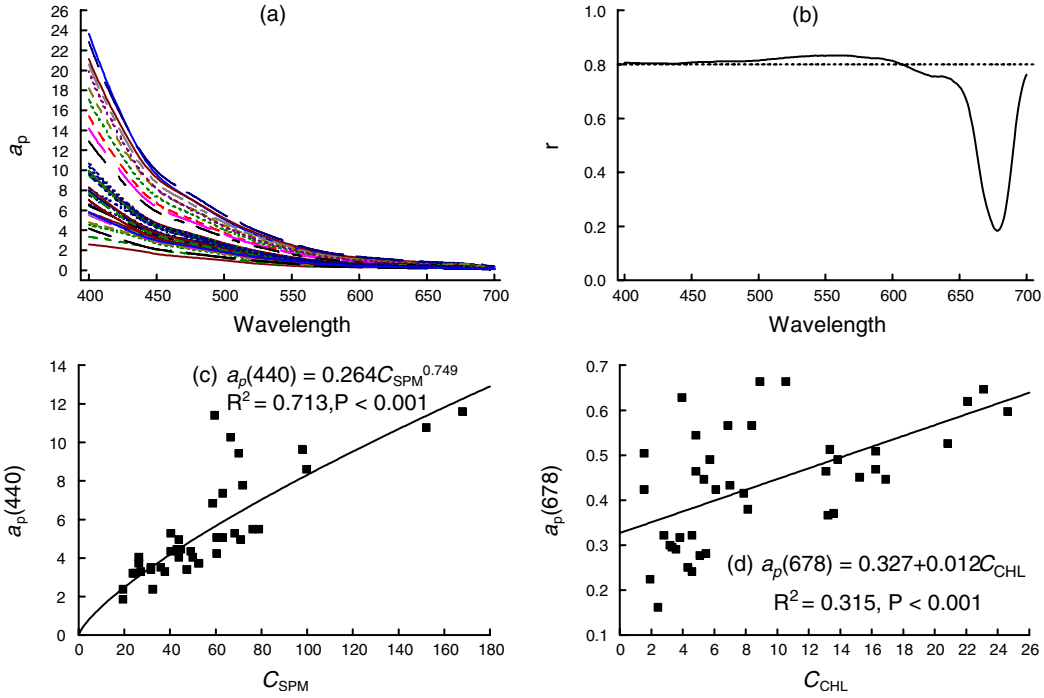

Fig. 5. (Color online) (a) Absorption coefficient of total particulate (a_p, m^{-1}) at wavelengths of 400–700 nm. (b) Correlation (r) between a_p and suspended particulate matter concentration (C_{SPM}, mg/l). (c) Regression between C_{SPM} and a_p at a wavelength of 440 nm [$a_p(440)$]. (d) Regression between chlorophyll a concentration (C_{CHL}, mg/l) and a_p at a wavelength of 678 nm [$a_p(678)$].

$P = 0.8886$) and reached the highest value at 676 nm ($r = 0.3$, $P = 0.0559$). Such results indicated that there was no significant correlation between a_g and C_{DOC} at wavelengths of 400–700 nm at a significance level of 0.05 for these 41 water samples, which could be explained by the low C_{DOC} and its variation. The results further showed there was no significant correlation between a_g and C_{SPM}, C_{SPIM}, C_{SPOM}, or C_{CHL} at a significance level of 0.05, which might also be because of the low C_{DOC} and its variation.

G. b_b

The backscattering coefficients of 41 water samples at six wavelengths of 420, 442, 470, 510, 590, and 700 nm are shown in Fig. 7(a). The b_b decreased with increasing wavelength at the wavelengths of 442–700 nm, and such a pattern is similar to that found in many lakes, such as Taihu Lake [30,54] and the Tamar estuary [17], while the b_b at 420 nm for some samples was lower than that at 470 nm, and such a pattern is also similar to the result of October 2008 in Taihu Lake [54].

The HydroScat-6 backscattering sensor was originally designed for measuring the backscattering coefficients of the Case 1 waters, and the corresponding correction method was also developed for Case 1 waters, in which the SPIM concentration is very low. When we applied this instrument in our study area, we found that the measurement values were not very steady, especially in the turbid waters, which possibly was caused by the multiscattering of SPIM. Therefore, we consider that the measurement uncertainties of the HydroScat-6 backscattering sensor and its subsequent correction method in turbid Case 2 waters might explain the result found in this study.

The results of the correlation analyses between b_b and the main water constituents are shown in Table 3. There existed strong and positive correla-

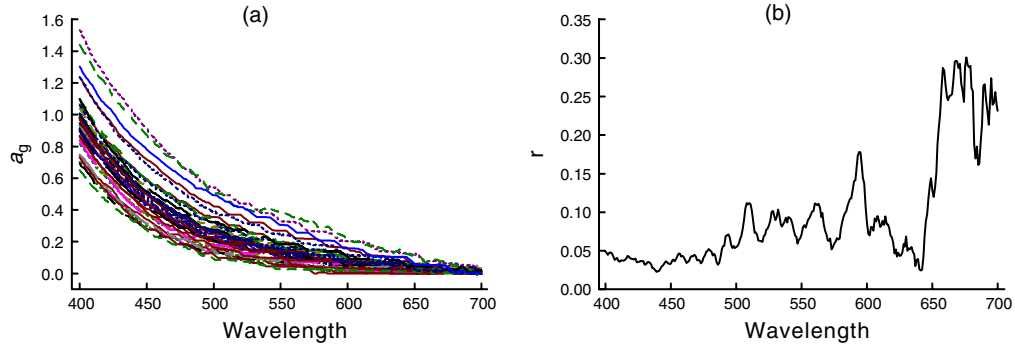

Fig. 6. (Color online) (a) Absorption coefficient of colored/chromophoric dissolved organic matter (a_g, m^{-1}), and (b) its correlation (r) to dissolved organic carbon concentration (C_{DOC}, mg/l) at wavelengths of 400–700 nm.

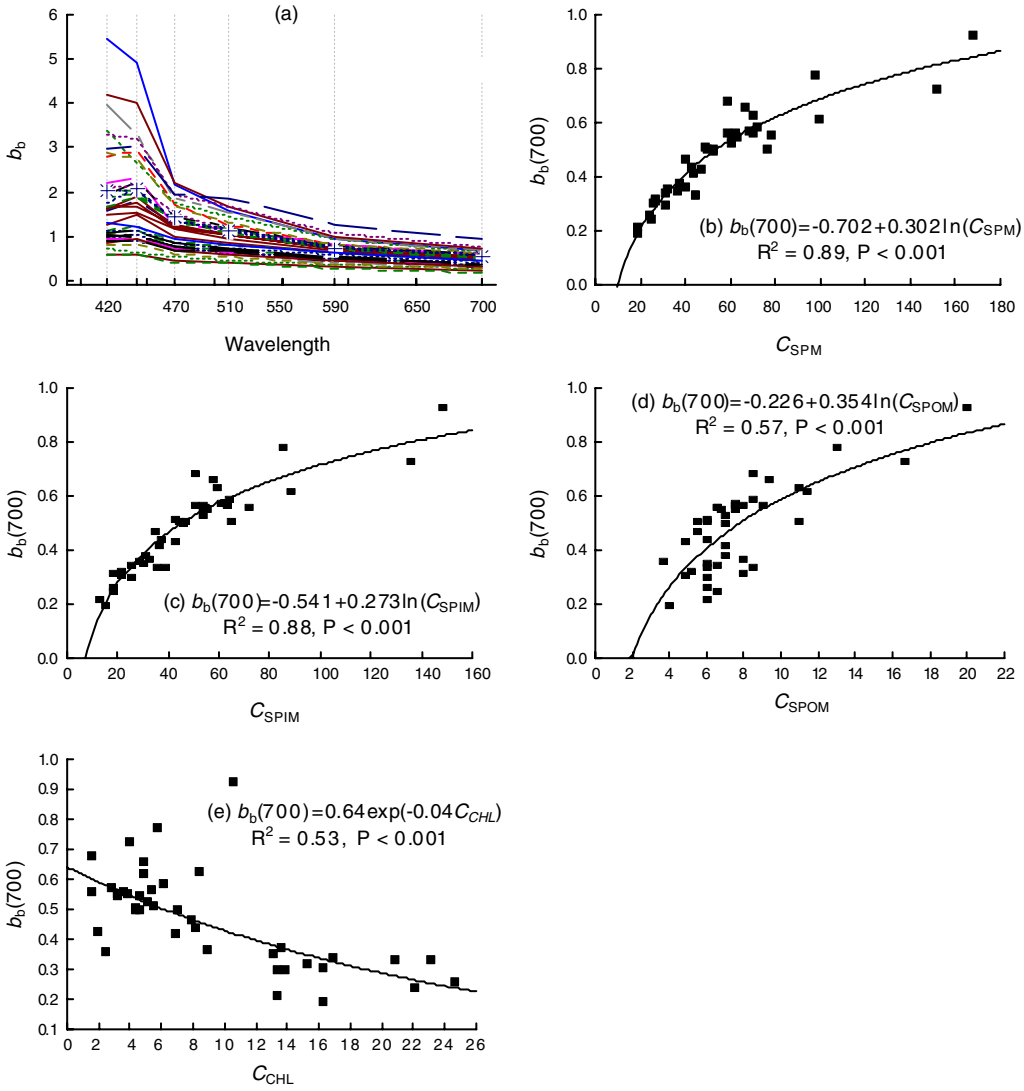

Fig. 7. (Color online) (a) Backscattering coefficient without the contribution of pure water (b_b, m^{-1}) at six wavelengths of 420, 442, 470, 510, 590, and 700 nm. (b) Regression between concentration of suspended particulate matter (C_{SPM}, mg/l) and b_b at a wavelength of 700 nm [$b_b(700)$]. (c) Regression between concentration of suspended particulate inorganic matter (C_{SPIM}, mg/l) and $b_b(700)$. (d) Regression between concentration of suspended particulate organic matter (C_{SPOM}, mg/l) and $b_b(700)$. (e) Regression between concentration of chlorophyll *a* (C_{CHL}, μg/l) and $b_b(700)$.

tions between b_b and C_{SPM}, C_{SPIM}, and C_{SPOM} at the six bands at a significance level of 0.05 due to the strong backscattering of nonpigment particulate, which is also similar to that found in Taihu Lake [30,54]. No correlation was found between b_b and C_{DOC} at a significance level of 0.05 for the weak backscattering of DOC. There were strong but negative correlations between b_b and C_{CHL} at the six bands at a significance level of 0.05, which is also similar to some of the results from Taihu Lake [54]. Phytoplankton, especially algae, contributes little to backscattering, and, thus, the weak and negative correlation between C_{SPM} and C_{CHL} [Fig. 2(a)] might explain indirectly the negative correlation between b_b and C_{CHL} because of the strong and positive correlation between b_b and C_{SPM}. The C_{SPM}, C_{SPIM}, C_{SPOM}, and C_{CHL} showed increasing correlations to b_b with increasing wavelength (Table 3), and they can explain 89%, 88%, 57%, and 53% of the variations of b_b at a wavelength of 700 nm [Figs. 7(b)–7(e)].

Table 3. Correlations Between Backscattering Coefficient of Water Constituents and Concentrations of Suspended Particulate Matter (C_{SPM}, mg/l), Suspended Particulate Inorganic Matter (C_{SPIM}, mg/l), Suspended Particulate Organic Matter (C_{SPOM}, mg/l), Dissolved Organic Carbon (C_{DOC}, mg/l), and Chlorophyll *a* (C_{CHL}, μg/l) of 41 Water Samples at Wavelengths of 420, 442, 470, 510, 590, and 700 nm[a]

Band	C_{SPM}	C_{SPIM}	C_{SPOM}	C_{DOC}	C_{CHL}
420	0.71	0.71	0.64	−0.10 [a]	−0.54
470	0.74	0.74	0.65	−0.10 [a]	−0.59
510	0.83	0.83	0.69	−0.17 [a]	−0.64
550	0.88	0.88	0.75	−0.14 [a]	−0.64
590	0.88	0.88	0.75	−0.12 [a]	−0.66
700	0.89	0.89	0.75	−0.12 [a]	−0.66

[a]Means no significant correlation at a significance level of 0.05.

4. Conclusion

This study of Poyang Lake reported the absorption and backscattering coefficients of the water body, and, further, analyzed their relations to the main water constituents. The principal results obtained for the particular sampling time period can be summarized as follows.

1. Poyang Lake is an SPIM-dominant lake with low phytoplankton concentration.
2. One obvious a_{ph} absorption peak was found at 678 nm, and it explained 72% of the variation of C_{CHL}.
3. The a_d and a_p exponentially decreased with increasing wavelength, and they explained 74% of the variation of C_{SPIM} and 71% of the variation of C_{SPM} at a wavelength of 440 nm.
4. The a_g also exponentially decreased with increasing wavelength, and it had no significant correlation to C_{DOC} at a significance level of 0.05.
5. The b_b decreased with increasing wavelength, and it had strong and positive correlations to C_{SPM}, C_{SPIM}, and C_{SPOM}; a strong and negative correlation to C_{CHL}; and no correlation to C_{DOC} at a significance level of 0.05.

However, such results can only represent the IOPs during the sampling time period, and more measurements and analyses in different seasons need to be carried out in the future to comprehensively understand the IOP dynamics of Poyang Lake.

This study was supported by the National Natural Science Foundation of China (NSFC, Grant No. 40971191), the Scientific Research Starting Foundation of the Ministry of Education of China for Returned Overseas Chinese Scholars, the Special Foundation of Ministry of Finance of China for Nonprofit Research of Forestry Industry (Grant No. 200904001) and the Knowledge Innovation Program of the Chinese Academy of Sciences (Grant No. KZCX2-YW-QN311).

References

1. A. Reinart, B. Paavel, D. Pierson, and N. Strombeck, "Inherent and apparent optical properties of Lake Peipsi, Estonia," Boreal Environ. Res. **9**, 429–445 (2004).
2. Z. P. Lee, K. L. Carder, and R. A. Arnone, "Deriving inherent optical properties from water color: a multiband quasi-analytical algorithm for optically deep waters," Appl. Opt. **41**, 5755–5772 (2002).
3. E. Leymarie, D. Doxaran, and M. Babin, "Uncertainties associated to measurements of inherent optical properties in natural waters," Appl. Opt. **49**, 5415–5436 (2010).
4. H. Loisel and D. Stramski, "Estimation of the inherent optical properties of natural waters from the irradiance attenuation coefficient and reflectance in the presence of Raman scattering," Appl. Opt. **39**, 3001–3011 (2000).
5. M. H. Pinkerton, G. F. Moore, S. J. Lavender, M. P. Gall, K. Oubelkheir, K. M. Richardson, P. W. Boyd, and J. Aiken, "A method for estimating inherent optical properties of New Zealand continental shelf waters from satellite ocean colour measurements," N. Z. J. Mar. Freshwater Res. **40**, 227–247 (2006).
6. E. H. S. Van Duin, G. Blom, F. J. Los, R. Maffione, R. Zimmerman, C. F. Cerco, M. Dortch, and E. P. H. Best, "Modeling underwater light climate in relation to sedimentation, resuspension, water quality and autotrophic growth," Hydrobiologia **444**, 25–42 (2001).
7. W. R. Clavano, E. Boss, and L. Karp-Boss, "Inherent optical properties of non-spherical marine-like particles—From theory to observation," Oceanogr. Mar. Biol. **45**, 1–38 (2007).
8. R. Ma, J. Tang, and J. Dai, "Bio-optical model with optimal parameter suitable for Taihu Lake in water colour remote sensing," Int. J. Remote Sens. **27**, 4305–4328 (2006).
9. T. Suresh, E. Desa, J. Kurian, and A. Mascarenhas, "Measurement of inherent optical properties in the Arabian Sea," Indian J. Mar. Sci. **27**, 274–280 (1998).
10. W. S. Pegau, "Inherent optical properties of the central Arctic surface waters," J. Geophys. Res. Oceans **107**, 8035 (2002).
11. G. Riccobene, A. Capone, S. Aiello, M. Ambriola, F. Ameli, I. Amore, M. Anghinolfi, A. Anzalone, C. Avanzini, G. Barbarino, E. Barbarito, M. Battaglieri, R. Bellotti, N. Beverim, M. Bonorl, B. Bouhadef, M. Brescia, G. Cacopardo, F. Cafagna, L. Caponetto, E. Castorina, A. Ceres, T. Chiarusi, M. Circella, R. Cocimano, R. Coniglione, M. Cordelli, M. Costa, S. Cuneo, A. D'Amico, G. De Bonis, C. De Marzo, G. De Rosa, R. De Vita, C. Distefano, E. Falchini, C. Fiorello, V. Flaminio, K. Fratini, A. Gabrielli, S. Galcotti, E. Gandolfi, A. Grimaldi, R. Habel, E. Leonora, A. Lonardo, G. Longo, D. Lo Presti, F. Lucarelli, E. Maccioni, A. Margiotta, A. Martini, R. Masullo, R. Megna, E. Migneco, M. Mongelli, T. Montaruli, M. Morganti, M. Musumeci, C. A. Nicolau, A. Orlando, M. Osipenko, G. Osteria, R. Papaleo, V. Pappalardo, C. Petta, P. Piattelli, F. Raffaelli, G. Raia, N. Randazzo, S. Reito, G. Kicco, M. Ripani, A. Rovelli, M. Ruppi, G. V. Russo, S. Russo, P. Sapienza, M. Sedita, J. P. Schuller, E. Shirokov, F. Simeone, V. Sipala, M. Spurio, M. Taiuti, G. Terreni, L. Trasatti, S. Urso, V. Valente, and P. Vicini, "Deep seawater inherent optical properties in the Southern Ionian Sea," Astropart. Phys. **27**, 1–9 (2007).
12. W. Ambarwulan, M. S. Salama, C. M. Mannaerts, and W. Verhoef, "Estimating specific inherent optical properties of tropical coastal waters using bio-optical model inversion and in situ measurements: case of the Berau estuary, East Kalimantan, Indonesia," Hydrobiologia **658**, 197–211 (2011).
13. D. McKee, A. Cunningham, J. Slater, K. J. Jones, and C. R. Griffiths, "Inherent and apparent optical properties in coastal waters: a study of the Clyde Sea in early summer," Estuarine Coastal Shelf Sci. **56**, 369–376 (2003).
14. M. S. Salama, A. Dekker, Z. Su, C. M. Mannaerts, and W. Verhoef, "Deriving inherent optical properties and associated inversion-uncertainties in the Dutch Lakes," Hydrol. Earth Syst. Sci. **13**, 1113–1121 (2009).
15. P. E. Lyon, F. E. Hoge, C. W. Wright, R. N. Swift, and J. K. Yungel, "Chlorophyll biomass in the global oceans: satellite retrieval using inherent optical properties," Appl. Opt. **43**, 5886–5892 (2004).
16. V. Balkanov, I. Belolaptikov, L. Bezrukov, N. Budnev, A. Capone, A. Chensky, I. Danilchenko, G. Domogatsky, Z. A. Dzhilkibaev, S. Fialkovsky, O. Gaponenko, O. Gress, T. Gress, R. Il'yasov, A. Klabukov, A. Klimov, S. Klimushin, K. Konischev, A. Koshechkin, V. Kuznetzov, L. Kumichev, V. Kulepov, B. Lubsandorzhiev, R. Masullo, E. Migneco, S. Mikheyev, M. Milenin, R. Mirgazov, N. Moselko, E. Osipova, A. Panfilov, L. Pan'kov, Y. Parfenov, A. Pavlov, M. Petruccetti, E. Pliskovsky, P. Pokhil, V. Poleschuk, E. Popova, V. Prosin, G. Riccobene, M. Rozanov, V. Rubtzov, Y. Semeney, C. Spiering, O. Streicher, B. Tarashansky, R. Vasiljev, R. Wischnewski, I. Yashin, and V. Zhukov, "Simultaneous measurements of

water optical properties by AC9 transmissometer and ASP-15 inherent optical properties meter in Lake Baikal," Nucl. Instrum. Methods Phys. Res. A **498**, 231–239 (2003).
17. D. Doxaran, N. Cherukuru, and S. J. Lavender, "Apparent and inherent optical properties of turbid estuarine waters: measurements, empirical quantification relationships, and modeling," Appl. Opt. **45**, 2310–2324 (2006).
18. G. Campbell, S. R. Phinn, and P. Daniel, "The specific inherent optical properties of three sub-tropical and tropical water reservoirs in Queensland, Australia," Hydrobiologia **658**, 233–252 (2011).
19. S. Sathyendranath, ed., "Remote sensing of ocean colour in coastal, and other optically-complex, waters," in Reports of the International Ocean-Colour Coordinating Group (International Ocean-Colour Coordinating Group, 2000).
20. J. T. O. Kirk, *Light and Photosynthesis in Aquatic Ecosystems* (Cambridge University, 1994).
21. C. E. Binding, J. H. Jerome, R. P. Bukata, and W. G. Booty, "Spectral absorption properties of dissolved and particulate matter in Lake Erie," Remote Sens. Environ. **112**, 1702–1711 (2008).
22. R. Ma, J. Tang, H. Duan, and D. Pan, "Progress in lake water color remote sensing," J. Lake Sci. **21**, 143–158 (2009) (in Chinese).
23. H. Loisel, X. Meriaux, A. Poteau, L. F. Artigas, B. Lubac, A. Gardel, J. Cafflaud, and S. Lesourd, "Analyze of the inherent optical properties of French Guiana coastal waters for remote sensing applications," J. Coastal Res. Special Issue **56**, 1532–1536 (2009).
24. W. Okullo, T. Ssenyonga, B. Hamre, O. Frette, K. Sorensen, J. J. Stamnes, A. Steigen, and K. Stamnes, "Parameterization of the inherent optical properties of Murchison Bay, Lake Victoria," Appl. Opt. **46**, 8553–8561 (2007).
25. D. Pan and R. Ma, "Several key problems of lake water quality remote sensing," J. Lake Sci. **20**, 139–144 (2008) (in Chinese).
26. N. Strombeck and D. C. Pierson, "The effects of variability in the inherent optical properties on estimations of chlorophyll *a* by remote sensing in Swedish freshwaters," Sci. Total Environ. **268**, 123–137 (2001).
27. D. Y. Sun, Y. M. Li, Q. Wang, J. Gao, H. Lv, C. F. Le, and C. C. Huang, "Light scattering properties and their relation to the biogeochemical composition of turbid productive waters: a case study of Lake Taihu," Appl. Opt. **48**, 1979–1989 (2009).
28. R. Ma, G. Yang, H. Duan, J. Jiang, S. Wang, X. Feng, A. Li, F. Kong, B. Xue, J. Wu, and S. Li, "China's lakes at present: number, area and spatial distribution," Sci. China Earth Sci. **54**, 283–289 (2011).
29. H. T. Duan, R. H. Ma, Y. Z. Zhang, S. A. Loiselle, J. P. Xu, C. L. Zhao, L. Zhou, and L. L. Shang, "A new three-band algorithm for estimating chlorophyll concentrations in turbid inland lakes," Environ. Res. Lett. **5**, 044009 (2010).
30. R. Ma, J. Tang, J. Dai, Y. Zhang, and Q. Song, "Absorption and scattering properties of water body in Taihu Lake, China: absorption," Int. J. Remote Sens. **27**, 4277–4304 (2006).
31. R. H. Ma, D. L. Pan, H. T. Duan, and Q. J. Song, "Absorption and scattering properties of water body in Taihu Lake, China: backscattering," Int. J. Remote Sens. **30**, 2321–2335 (2009).
32. C. F. Le, Y. M. Li, Y. Zha, D. Y. Sun, and B. Yin, "Validation of a quasi-analytical algorithm for highly turbid eutrophic water of Meiliang Bay in Taihu Lake, China," IEEE Trans. Geosci. Remote Sens. **47**, 2492–2500 (2009).
33. Y. L. Zhang, B. Zhang, X. Wang, J. S. Li, S. Feng, Q. H. Zhao, M. L. Liu, and B. Q. Qin, "A study of absorption characteristics of chromophoric dissolved organic matter and particles in Lake Taihu, China," Hydrobiologia **592**, 105–120 (2007).
34. Q. Wang, X. Jin, Y. Li, C. Wu, H. Lü, Y. Wang, H. Zhang, B. Yin, and L. Zhu, "Estimation of suspended sediment concentration based on bio-optical mechanism and HJ-1 image in Chaohu Lake," Sci. China Earth Sci. **53**, 58–66 (2010).
35. Q. Min, "On the regularities of water level fluctuations in Poyang Lake," J. Lake Sci. **7**, 281–288 (1995) (in Chinese).
36. D. Xu, M. Xiong, and J. Zhang, "Analysis on hydrologic characteristics of Poyang Lake," Yangtze River **32**, 21–27 (2001).
37. D. Shankman, B. D. Keim, and J. Song, "Flood frequency in China's Poyang Lake region: trends and teleconnections," Int. J. Climatol. **26**, 1255–1266 (2006).
38. Y. Wu and W. Ji, *Study on Jiangxi Poyang Lake National Nature Reserve* (Forest Publishing, 2002).
39. G. Huang, "On ecological security and ecological construction of Poyang Lake district," Sci. Technol. Rev. **24**, 73–78 (2006) (in Chinese).
40. L. Zhen, F. Li, H. Huang, O. Dilly, J. Liu, Y. Wei, L. Yang, and X. Cao, "Households' willingness to reduce pollution threats in the Poyang Lake region, southern China," J. Geochem. Explor. **110**, 15–22 (2011).
41. X. Deng, Y. Zhao, F. Wu, Y. Lin, Q. Lu, and J. Dai, "Analysis of the trade-off between economic growth and the reduction of nitrogen and phosphorus emissions in the Poyang Lake Watershed, China," Ecolog. Model. **222**, 330–336 (2011).
42. Y. Zhong and S. Chen, "Impact of dredging on fish in Poyang Lake," Jiangxi Fish. Sci. Technol. **1**, 15–18 (2005) (in Chinese).
43. G. Wu, J. De Leeuw, A. K. Skidmore, H. H. T. Prins, and Y. Liu, "Concurrent monitoring of vessels and water turbidity enhances the strength of evidence in remotely sensed dredging impact assessment," Water Res. **41**, 3271–3280 (2007).
44. H. T. Duan, R. H. Ma, J. P. Xu, Y. Z. Zhang, and B. Zhang, "Comparison of different semi-empirical algorithms to estimate chlorophyll-a concentration in inland lake water," Environ. Monit. Assess. **170**, 231–244 (2010).
45. M. Laanen, "Yellow matters: improving the remote sensing of coloured dissolved organic matter in inland freshwaters," Ph.D. dissertation (VU University, Amsterdam, 2007).
46. J. S. Cleveland and A. D. Weidemann, "Quantifying absorption by aquatic particles: a multiple scattering correction for glass-fiber filters," Limnol. Oceanogr. **38**, 1321–1327 (1993).
47. A. Bricaud, A. Morel, and L. Prieur, "Absorption by dissolved organic matter of the sea (yellow substance) in the UV and visible domains," Limnol. Oceanogr. **26**, 43–53 (1981).
48. D. J. Keith, J. A. Yoder, and S. A. Freeman, "Spatial and temporal distribution of coloured dissolved organic matter (CDOM) in Narragansett Bay, Rhode Island: implications for phytoplankton in coastal waters," Estuarine Coastal Shelf Sci. **55**, 705–717 (2002).
49. HOBI Labs Inc., "Backscattering sensor calibration manual (Revision N)" (2008).
50. C. Le, Y. Li, Y. Zha, and D. Sun, "Specific absorption coefficient and the phytoplankton package effect in Lake Taihu, China," Hydrobiologia **619**, 27–37 (2009).
51. V. Stuart, S. Sathyendranath, T. Platt, H. Maass, and B. D. Irwin, "Pigments and species composition of natural phytoplankton populations: effect on the absorption spectra," J. Plankton Res. **20**, 187–217 (1998).
52. C. S. Roesler, M. J. Perry, and K. L. Carder, "Modeling in situ phytoplankton absorption from total absorption spectra in productive inland marine waters," Limnol. Oceanogr. **34**, 1510–1523 (1989).
53. W. Cao, Y. Yang, X. Xu, L. Huang, and J. Zhang, "Regional patterns of particulate spectral absorption in the Pearl River estuary," Chin. Sci. Bull. **48**, 2344–2351 (2003).
54. R. Ma, H. Duan, J. Tang, and Z. Chen, *Remote Sensing of Lake Water Environment* (Science, 2010) (in Chinese).